# Highly efficient and recyclable monolithic bioreactor for interfacial enzyme catalysis

Zhengqiao Yin,[a] Yiding Zhou,[a] Xiucai Liu,[a] Shengmiao Zhang,*[a] and Bernard P. Binks*[b]

[a]*Shanghai Key Laboratory of Advanced Polymeric Materials, Key Laboratory for Ultrafine Materials of Ministry of Education, School of Materials Science and Engineering, East China University of Science and Technology, Shanghai 200237, China*

[b]*Department of Chemistry, University of Hull, Hull. HU6 7RX. UK*

* Corresponding authors: shmzhang@ecust.edu.cn; b.p.binks@hull.ac.uk

**Keywords:** Pickering emulsion, emulsion-template, monolithic bioreactor, polymersome, biphasic biocatalyst

**Abstract**

Hypothesis

Biocatalysts are key to the realization of all bioconversions in nature. However, the difficulty of combining the biocatalyst and other chemicals in one system limits their application in artificial reaction systems. Although some effort, such as Pickering interfacial catalysis and enzyme-immobilized microchannel reactors, have addressed this challenge an effective method to combine chemical substrates and biocatalysts in a highly efficient and re-usable monolith system is still to be developed.

Experiments

A repeated batch-type biphasic interfacial biocatalysis microreactor was developed using enzyme-loaded polymersomes in the void surface of porous monoliths. Polymersomes, loaded with Candida antarctica Lipase B (CALB), are fabricated by self-assembly of the copolymer PEO-*b*-P(St-*co*-TMI) and used to stabilize oil-in-water (o/w) Pickering emulsions as a template to prepare monoliths. By adding monomer and Tween 85 to the continuous phase, controllable open-cell monoliths are prepared to inlay CALB-loaded polymersomes in the pore walls.

Findings

The microreactor is proven to be highly effective and recyclable when a substrate flows through it, which offers superior benefits of absolute separation to a pure product and no enzyme loss. The relative enzyme activity is constantly maintained above 93% in 15 cycles. The enzyme is constantly present in the microenvironment of the PBS buffer ensuring its immunity to inactivation and facilitating its recycling.

## 1. Introduction

As the key to realizing all biological transformations in nature, biocatalysts have long been valued by various application fields from academia to industry due to their versatility, high selectivity, reaction purity and broad substrate spectrum [1]. However, up to now, biocatalysts hold only a small share of the huge catalytic market, because it is difficult to combine biocatalysts and chemicals in one system. Most biocatalysts are most active in aqueous media, while most chemicals have poor water solubility. Therefore, the reaction can only run in organic environments. This is a natural contradiction. What's more, there is a serious problem that the enzyme is difficult to purify after the reaction. Therefore, it is important to explore an effective method to combine chemical substrates and biocatalysts in one system such that the enzyme is not affected by the separation of water and oil after the reaction.

So far, one of the most prevalent approaches of using biocatalysts in organic media has been the use of emulsions which involves both organic and aqueous phases. For example, Pickering interfacial catalysis (PIC) has been developed [2, 3]. PIC is typically achieved by using catalytically active micro-/nanoparticles to stabilize emulsions (so-called Pickering emulsions) for interfacial reactions [4, 5]. In PIC, covalently immobilized enzyme particles are prepared as the stabilizer of a Pickering emulsion [6-9]. More recently, to avoid any negative effect on the structure of an enzyme caused by covalent immobilization, non-covalently immobilized enzyme approaches such as encapsulating it inside vesicles, has also been reported as the stabilizer of the PIC system [10]. In those approaches, the Pickering emulsions normally need to be demulsified and separated by adding extra components or centrifuged to recycle the enzyme immobilized nanoparticles. However, complete recycling of the enzyme is difficult to achieve.

Moreover, biphasic reactions usually require external mechanical stirring to mix the two phases and provide a large reaction area during the workup, which must be carried out in a batch reactor. In terms of convenience for practical use, a flow-through process has obvious advantages in productivity, mixing efficiency, safety and process

control [11]. Therefore, it is highly desirable to develop a more straightforward and practical system to convert the biphasic reaction from a batch mode to a flow-through fashion. Enzyme-immobilized microchannel reactors seem a good solution [12, 13]. Compared with typical batch methods, process intensification using microchannel reactors has significant advantages, such as rapid mass and heat transfer and large surface area to volume ratio. These advantageous features are also found in the catalytic reactions conducted in a microreactor with enzymes immobilized on its channels' inner walls, *e.g.* as an enzyme-immobilized polymeric membrane. α-chymotrypsin buffer solution was mixed with glutaraldehyde and formaldehyde as cross-linkers in a commercial PTFE tube of diameter 500 μm [14, 15]. Consequently, a cross-linked enzyme aggregate (CLEA) membrane was formed on the inner walls of the tube. When an electronegative enzyme was used, fast and efficient CLEA formation could be achieved by co-precipitation of the enzyme with poly-L-lysine [15]. The enzyme-immobilized microchannel reactors clearly have great potential for designing sustainable and green biotransformations. Littlechild *et al*. reported a different method [16]. In their work, CLEAs were fabricated from a *Thermococcus litorali* derived thermophilic L-aminoacylase. The enzymes had been overexpressed in *E. Coli.* The CLEAs were trapped by frits in the microfluidic channels in capillary flow reactors. However, CLEA as a covalent immobilizing method may cause a negative influence on the structure of the enzyme. The best means of avoiding any negative influence is to encapsulate it [6].

The enzyme-immobilized support is the primary challenge in enzyme immobilization. Currently, porous supports are most employed to immobilize enzymes [17, 18]. The method of immobilization and the porous structure of the supports largely determine the specific activity and stability of the immobilized enzyme. The mass transfer during catalysis is also influenced by the void diameter and interconnectivity of the porous material. Emulsion-templated monoliths with hierarchical and tunable porous structure have received increasing attention in recent years for enzyme immobilization [19]. Huang *et al*. adsorbed Laccase on chitin/graphene oxide (Ch/GO)

beads through a Pickering emulsion template method [20], and then cross-linked them with glutaraldehyde. The Laccase-loaded Ch/GO beads demonstrated remarkable catalytic performance and enzyme stability for dye decolorization. However, the cross-linking reaction disrupts the spatial structure of the enzyme resulting in irreversible deactivation. We immobilized CALB onto the surface of the void walls of emulsion-templated beads and ZIF-8 nanoparticles [21, 22]. The immobilized enzyme was then used to catalyze the hydrolysis of 4-nitrophenyl palmitate. In these previous works, the enzyme was exposed to organic solvents during the reaction which could cause its deactivation.

In this work, we report a Pickering emulsion-templated monolith having its walls decorated with enzyme-loaded polymersomes. Along with the substrate (*p*-NPB in *n*-heptane) flowing through it, the monolith exhibited excellent biocatalytic performance for hydrolysis and outstanding re-usability. The polymersomes herein not only protect the enzyme from deactivation and provide sites for enzymatic reaction, but also act as the stabilizer of the emulsion template before it solidifies into a porous material (Scheme 1). Generally, in an emulsion-templated technique, a high internal phase emulsion (HIPE) is used as a template [23, 24]. If the HIPE is stabilized by particles rather than surfactant, it is called a Pickering HIPE [25, 26]. With Pickering HIPE as a template, the resulting porous materials (polyHIPPE) obtained by curing its continuous phase are functionalized by the Pickering emulsion stabilizer with enzyme immobilized in the surface of voids. Based on the above phenomena, we design and prepare an enzyme-loaded polymersome as a stabilizer for Pickering HIPEs and therefore enable the resulting monolith to be a high-throughput enzymatic microreactor. Benefiting from the uniquely embedded structure of polymersomes within the void surface, the microreactor combines the advantages of polyHIPPE with interfacial biocatalysis, thus achieving a solid-state biphasic catalysis by exploiting colloidal properties. The interconnecting microchannels in the polyHIPPE hierarchical structure also conform with Murray's law hence are ideal for heat and mass transport of mixed liquids [27]. Compared with enzyme-immobilized Pickering emulsions [5, 9, 28], the monolithic

microbioreactor as a solid support material can be completely separated from the substrate leading to no loss of enzyme. The enzyme is protected within polymersomes from the organic medium and consequently retains its activity during multiple enzymatic reaction cycles.

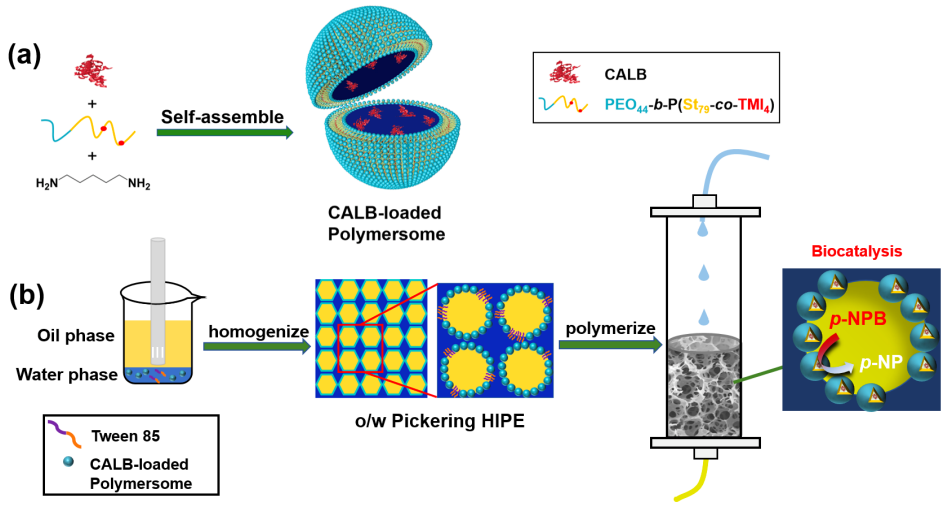


**Scheme 1.** Preparation of emulsion-templated biocatalytic reactor and its catalytic process. (a) Fabrication of CALB-encapsulated polymersomes, (b) preparation of o/w Pickering emulsion-templated monolith and enzymatic reaction within it.

## 2. Materials and methods

### 2.1 Materials

Methoxypolyethylene glycol (MePEO, $M_n$ = 2000 g/mol, PDI = 1.09), 4-dimethylaminopyridine (DMAP, 99%), α-bromophenylacetic acid (99.9%), *n*-hexane (98%), methanol (99.9%) and *p*-toluenesulfonic acid (PTSA, 99%) were purchased from Macklin Biochemical Co., Ltd. (Shanghai). Toluene (99.5%), benzene (99%), dichloromethane (DCM, 99%), 1,2-dichloroethane (DCE, 99%) and tetrahydrofuran (THF, 99%) were obtained from Shanghai Titan Scientific Chemical Regent Co. Ltd. and were dried with 4Å molecular sieve before use. *n*-heptane (99%), *p*-nitrophenol butyrate (99.5%, *p*-NPB), sodium phosphate dibasic dodecahydrate (99.5%), *p*-nitrophenol (*p*-NP, 99%) and potassium dihydrogen phosphate (99.5%) were purchased from Shanghai Titan Scientific Chemical Regent Co. Ltd. Phenylmagnesium bromide

(1.0 M solution in THF), carbon disulfide (99%), dicyclohexylcarbodiimide (DCC, 99%), 3-isopropenyl-α,α-dimethylbenzyl isocyanate (TMI, 99%), 2,2-azobis(2-methylpropionitrile) (AIBN, 99%) and 1,5-pentanediamine were bought from Aladdin (Shanghai). Styrene (St, 99%, Shanghai Titan Scientific Chemical Reagent Co. Ltd.) was purified by filtration through basic and neutral alumina. Acrylamide (AM, 99%), N,N′-methylene bisacrylamide (MBAM, 99%), N,N,N,N-tetramethylethylenediamine (TMEDA, 99%) and Tween 85 (99.9%) were purchased from Macklin Biochemical Co., Ltd (Shanghai). Fluorescein isothiocyanate (FITC, 99%, Solarbio Science & Technology Co. Ltd., Beijing), Rhodamine B (99%, Yuanye Bio-Technology Co., Ltd. Shanghai), Lipozyme® CALB (6%, Novozymes, Biotechnology Co. Ltd., China) were used as received. PBS buffer (40 mM, pH = 8) was prepared in the lab. Potassium persulfate (KPS, 99.5%, Shanghai Titan Scientific Chemical Regent Co. Ltd.) was recrystallized twice before use. A Bicinchoninic Acid Kit for protein determination (BCA kit) and 96-well flat bottom transparent microtiter plates were purchased from Beyotime Biochemical Co. Ltd. (Shanghai). Ultrapure water (Milli-Q, resistivity 18.2 mΩ cm) was used.

### 2.2 Preparation and characterization of $PEO_{44}$-*b*-P($St_{79}$-*co*-$TMI_4$) copolymer

Polymersomes are commonly obtained by self-assembly from amphiphilic copolymers [29, 30]. Herein, an amphiphilic copolymer of PEO-*b*-P(St-*co*-TMI) is to be synthesized *via* RAFT polymerization as the building unit for constructing polymersomes [10]. The preparation and characterization of the PEO macro-chain transfer agent (PEO-CTA) is described in the Supporting Information. The synthesis of $PEO_{44}$-*b*-P($St_{79}$-*co*-$TMI_4$) is as follows.

St (1.9 g, 18.3 mmol), TMI (193 mg, 0.96 mmol), AIBN (2 mg, 0.012 mmol) and synthesized PEO-CTA (174 mg, 0.06 mmol) were added to a 25 ml three-neck flask. A Schlenk line was employed to degas the solution *via* four circular freeze-pump-thaw processes. Afterwards, the solution was stirred for 10 h at 75 ℃ under a nitrogen atmosphere before it was quickly cooled down with an ice-methanol bath. The solution

was added dropwise to 300 ml of methanol at 4 °C and a sediment was obtained as a pink solid. The crude product was further precipitated an additional two times and a purified product was obtained after freeze-drying. The yield was 67%. The obtained $PEO_{44}$-*b*-P($St_{79}$-*co*-$TMI_4$) copolymer was determined by FT-IR (Nicolet 6700), $^1$H-NMR (AvanceIII 500 MHz) and GPC (Waters 1515). $^1$H-NMR (500 MHz, $CDCl_3$) δ = 1.27-1.82 (m, $CH_2$, CH, $CH_3$), 3.38 (s, 3H, $CH_3OCH_2$), 3.60-3.66 (m, $OCH_2$), 6.46-7.09 (br. s, arom. H). FT-IR: 3058, 3025, 2921, 2252 (νN=C=O), 1601, 1493, 1451, 1109, 755, 696 $cm^{-1}$. $M_n$ = 15 kDa, PDI = $M_z/M$ = 1.29.

### 2.3 Preparation and characterization of CALB-loaded polymersomes

CALB-loaded polymersomes were prepared as follows. 100 mg of $PEO_{44}$-*b*-P($St_{79}$-*co*-$TMI_4$) was dissolved in 20 ml of THF in a flask and 5 ml of PBS buffer containing 15 mg of CALB was injected into the solution with a plunger pump at a rate of 0.08 ml $min^{-1}$. Subsequently, 15 ml of PBS buffer was added dropwise to the mixture. Afterwards, the solution was stirred for 30 min at room temperature before 60 µl of 1,5-pentanediamine was added. The mixture was shaken for 3 h within a shaking incubator. It was finally dialyzed against PBS buffer to remove both THF and excess 1,5-pentanediamine with dialysis tubing of 7,000 Da. The obtained solution was centrifuged (6,000 rpm, 10 min) to recover the polymersomes and the obtained polymersomes were re-dispersed in PBS buffer three times to wash off free enzyme. Finally, the polymersome concentration in PBS buffer was adjusted to 50 mg $ml^{-1}$. The preparation of polymersomes without CALB is described in the Supporting Information.

The cross-linking progress of polymersomes was detected by FT-IR. The mean particle size and polydispersity of the resulting polymersomes with and without CALB were characterized by dynamic light scattering (DLS), and the morphology of them was determined by SEM and TEM. The presence of CALB within polymersomes was verified by labelling using a fluorescent marker of FITC, and the encapsulation content of CALB in the polymersomes was determined by the BCA method. Detailed information of the characterization is given in the Supporting information.

### 2.4 Preparation and characterization of CALB-loaded monolith

CALB-loaded monoliths were prepared as follows. An aqueous phase was prepared by dissolving AM (0.4 g), MBAM (0.04 g) and KPS (0.02 g) in 2 ml of PBS buffer containing CALB-loaded polymersomes. Then 8.0 ml of *n*-heptane as the oil phase was added to the aqueous phase with emulsification using an Ultra Turrax T18 homogenizer at 8,000 rpm for 2 min to obtain an oil-in-water (o/w) Pickering HIPE. TMEDA (0.02 g) was added to the emulsion which was homogenized for another 5 sec. The prepared emulsion was then quickly transferred to a chromatographic column (height × inner diameter, 150 mm × 18 mm). TMEDA and KPS were used as a redox pair to allow the polymerization to occur under mild conditions [31]. Finally, an enzyme immobilized monolith polyHIPPE (named PPH-0) was obtained by polymerizing monomer in the aqueous phase for 24 h at 35 ℃ in an oven. The height of the final cylindrical monolith was around 40 mm.

The monolith obtained from the Pickering HIPE stabilized solely by particles would be closed-cell [32]. In order to obtain an open-cell porous monolith, a small amount of surfactant is commonly added as a co-stabilizer of the Pickering emulsion template [33, 34]. Herein, various amounts (40, 80 or 120 mg) of Tween 85 were added as co-stabilizer. The solid macroporous products were washed with PBS buffer to remove the oil phase and Tween 85 for further use. The open-cell enzyme-loaded monoliths were named PPH-2, PPH-4 and PPH-6 depending on the content of Tween 85 relative to PBS buffer (Table S1).

The templates of Pickering HIPEs were observed using confocal laser scanning microscopy (CLSM), before which the aqueous phase was dyed with Rhodamine B. The enzyme location was observed using CLSM *via* FITC-labelled CALB-loaded polymersomes stabilizing Pickering HIPEs. The morphology of CALB-loaded monoliths was analysed by SEM, and characterization of the porosity and interconnectivity is described in the Supporting Information.

### 2.5 Enzyme specific catalytic activity for biocatalytic reactor

The internal phase *n*-heptane in polymerized open-cell monoliths was removed by washing with PBS solution, and the monoliths were then used as a biocatalytic reactor without drying. The continuous-flow biocatalytic reaction in the reactor was carried out as follows: 12 ml of *n*-heptane containing the substrate *p*-NPB (25 mM) and 15 ml of PBS buffer were added to a 100 ml conical flask. For the first catalytic loop, the upper layer (*p*-NPB in *n*-heptane solution) of the immiscible two-phase mixture was pumped onto the monolith using a peristaltic pump, and allowed to flow by gravity through it at room temperature. After all the oil was added, the lower PBS buffer layer was then pumped into the monolith to take out both the *n*-heptane and water-soluble product *p*-NP to the flask below the column since the emulsion-templated monolith could be an efficient micromixer [35, 36]. The flow rate of the substrate in the monolith is determined by calibrating the flow rate of the peristaltic pump as 1.5 ml per min. Phase separation occurred quickly between *n*-heptane and PBS buffer as they were collected in the flask. The above operations are then repeated and the second and subsequent loops were executed. The enzyme specific catalytic activity for free CALB is described in the Supporting Information. The product *p*-NP was determined by measuring its absorbance at a wavelength of 405 nm with a microplate reader (SpectraMax M2), and the enzyme specific activity (U) is defined as 1 μmol *p*-NP product produced within 1 min. The operation was repeated three times for each catalytic process and the amount of *p*-NP was determined by averaging three groups of the absorbance.

### 2.6 Recyclability of CALB-loaded monolith

The monoliths were used for repeated enzymatic hydrolysis by adding the same amount of substrate *p*-NPB. After every biocatalytic cycle, the monolith was washed with excess PBS buffer to remove residual *p*-NPB and *p*-NP. The generated amount of *p*-NP in PBS after each cycle was measured by the microplate reader. Each cycle of catalysis was repeated for three times and taken as an average.

## 3. Results and Discussion

### 3.1 Preparation and characterization of enzyme-loaded polymersomes

#### 3.1.1 Synthesis of PEO-CTA and $PEO_{44}$-*b*-P($St_{79}$-*co*-$TMI_4$)

Enzyme-encapsulated polymersomes were required to act as both the sites for the enzymatic reaction and the stabilizer of the emulsion template, as well as the protector of the enzyme from organic reaction media. Hence, an amphiphilic block copolymer of PEO-*b*-P(St-*co*-TMI) was synthesized *via* RAFT polymerization to be a building block for the construction of polymersomes to encapsulate a model lipase CALB.

PEO-*b*-P(St-*co*-TMI) was synthesized as illustrated in Scheme S1 and S2 in the Supporting Information. First, the catalyst 4-(Dimethylamino)pyridinium-4-toluenesulfonate (DPTS) was obtained with PTSA and DMAP–as reactants (Figure S1) [37]. PEO macro-chain transfer agent (PEO-CTA) was synthesized in a two-step process by end group modification, including esterification of monomethoxy PEO with α-bromophenylacetic acid to α-bromo-phenylacetate terminated PEO and the synthesis of PEO macro-chain transfer agent with dithioester which was coupled by phenylmagnesium bromide and carbon disulfide (Scheme S1) [38]. As shown in Figure S2, $^1$H-NMR was used to characterize the end functionalization of PEO-CTA and the aromatic protons ortho to the C=S group were at 8.00-8.02 ppm for the dithioester group.

Then, the copolymer $PEO_{44}$-*b*-P($St_{79}$-*co*-$TMI_4$) was fabricated at 70 ℃ with RAFT polymerization in the presence of PEO-CTA (Scheme S2). As shown in the $^1$H-NMR characterization, characteristic peaks of PS-*co*-TMI groups were at 1.27-1.82 ppm and the phenyl ring was at 6.46-7.09 ppm, while peaks of aromatic protons ortho to the C=S group disappeared (Figure S3). In the FT-IR characterization of the block copolymer (Figure S4), 3058 and 3025 $cm^{-1}$ are C-H stretching vibration peaks on unsaturated carbon atoms, 2252 $cm^{-1}$ is the stretching vibration peak of the anchor group of N=C=O in TMI and the group of C=C stretching vibration is at 1601 $cm^{-1}$. The polydispersity

index of the block copolymer was 1.29 characterized by GPC, which shows a narrow molecular weight distribution for use as a building block [39].

### 3.1.2 Preparation of enzyme-loaded polymersomes

Amphiphilic copolymers with a narrow molecular weight distribution have been shown to be good building blocks for the construction of polymersomes through self-assembly [40]. Herein, CALB-loaded polymersomes were prepared first by dissolution of $PEO_{44}$-*b*-P($St_{79}$-*co*-$TMI_4$) in THF, which is favourable for both hydrophilic (core) and hydrophobic (corona) blocks. The self-assembly fabrication procedure of polymersomes is shown in Scheme 1(a). When PBS buffer containing CALB was added as a precipitant for the hydrophobic block P($St_{79}$-*co*-$TMI_4$), self-assembly occurred and CALB was encapsulated in the polymersomes [41]. Addition of PBS buffer was resumed to allow aggregation to a sphere and maintain the morphology. The inherent isocyanate group TMI cross-linked with external 1,5-pentanediamine, which was dripped in before the polymersome dispersion vibrated for 3 h to make the polymersomes robust and prevent the escape of CALB. The cross-linking was confirmed by FT-IR analysis (Figure S5). Compared to the uncross-linked polymersome, the vibration for the isocyanate moiety at 2254 $cm^{-1}$ disappeared whereas the urea peaks at 1538 $cm^{-1}$ and 1654 $cm^{-1}$ were detected after cross-linking. The construction of polymersomes with or without CALB was proved by both SEM and TEM analysis (Figure 1). The polymersomes had a hollow structure and smooth surfaces (Figure 1(b), 1(f)). Some polymersomes are broken due to the ultra-high vacuum of the electron microscopes but it allows us to demonstrate their hollow nature. From the TEM images (Figure 1(c), (g)), the presence of CALB seems to have no effect on the membrane thickness of polymersomes. DLS analysis showed that both the CALB-loaded polymersomes and those without CALB had a narrow particle size polydispersity of 0.21 and 0.13, respectively (Figure 1(a), (e)). Moreover, the mean diameter of CALB-loaded polymersomes (639 ± 155 nm) was similar to that of polymersomes without CALB (607 ± 132 nm). Both kinds of polymersome retained their structure for more than 100 days (Figures S6 and S7), indicating that they are

physically stable as a microencapsulation carrier and may act as the stabilizer for Pickering emulsions.

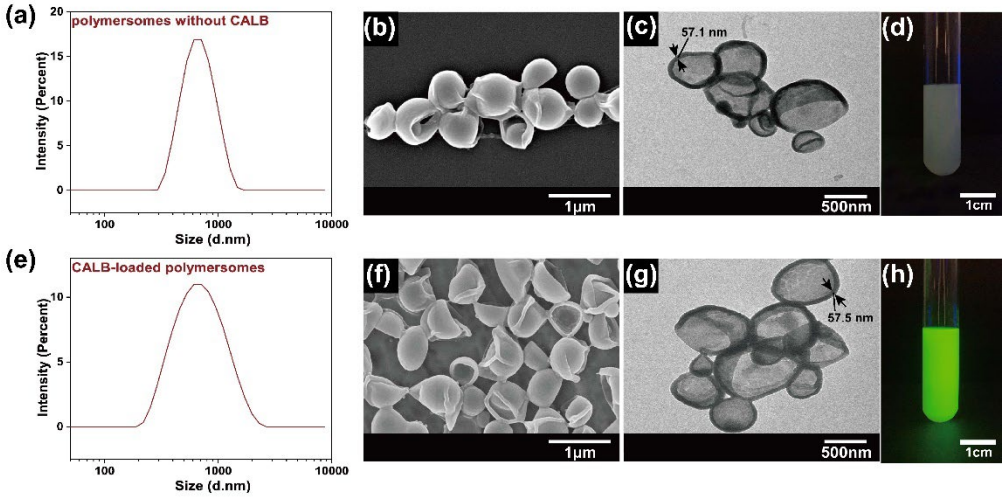


**Figure 1**. Size distributions, SEM images and TEM images respectively of cross-linked polymersomes (a)-(c) without CALB and (e)-(g) with CALB. Photos of aqueous polymersome dispersion under UV light (λ = 365 nm) (d) without CALB and (h) with CALB (h). CALB was labelled with FITC after loading.

To further verify the success of loading CALB into polymersomes, FITC was used to label the encapsulated CALB. The N=C=S group of FITC can tightly combine with amino groups of the lysine of CALB in alkaline solution and show green fluorescence under UV light of 365 nm [42]. As shown in Figure 1(d) and 1(h), when the CALB-loaded polymersome aqueous dispersion was exposed to UV light, it displayed bright green fluorescence whereas the polymersome without CALB aqueous dispersion had no fluorescence, proving that the enzyme was successfully encapsulated in polymersomes. The quantitative analysis of CALB in polymersomes was determined by the BCA method. The concentration of CALB was calculated from the absorbance at λ = 562 nm using a microplate reader and compared with the calibration curve (Figure S8). Enzyme loading content was calculated up to 9.1 ± 0.5 wt.% in the CALB-loaded polymersomes with an immobilization efficiency of 60 ± 3%.

### 3.2 Pickering emulsion-templated monolith

The enzyme-loaded polymersomes were expected to be a stabilizer of Pickering HIPE templates and subsequently biocatalysis sites of the resulting monolith. The obtained CALB-loaded polymersomes were used to stabilize Pickering HIPEs, which was further used as the template to fabricate the porous monolith by curing the continuous phase as shown in Scheme 1(b). Firstly, a *n*-heptane-in-water (o/w) Pickering HIPE with an internal phase ratio of 80 vol.% was prepared with 5 wt.% CALB-loaded polymersomes in water. The Pickering HIPE (HIPE-0) could withstand being inverted even 20 days after it was prepared (Figure S9). The extreme stability of this HIPE makes it a good candidate as an emulsion template for the synthesis of porous materials [43].

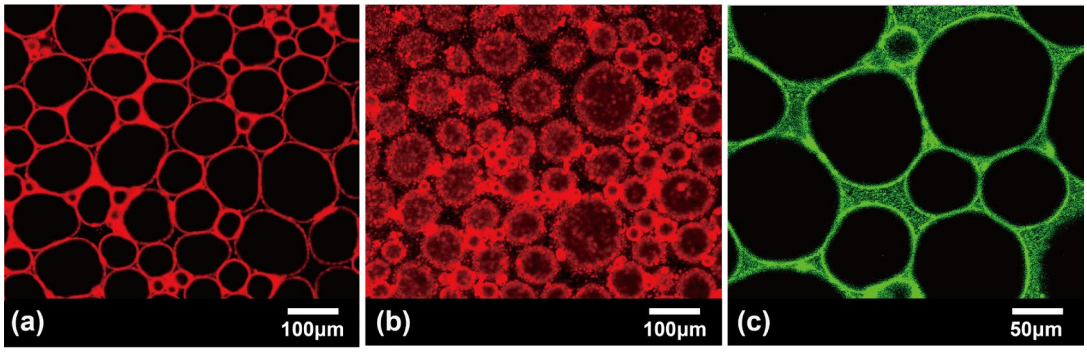


**Figure 2**. CLSM images of o/w Pickering HIPE-0 stabilized by 5 wt.% CALB-loaded polymersomes. (a), (b) Aqueous phase was dyed with Rhodamine B before emulsification and excited by light of $\lambda = 561$ nm at different focal lengths, (c) CALB inside polymersomes was labelled with FITC and excited by light of $\lambda = 488$ nm.

The type of emulsion was determined by CLSM. Before observation, the aqueous phase was dyed with a water-soluble fluorescence reagent Rhodamine B. The prepared Pickering HIPE was excited by light of wavelength 561 nm. As shown in Figure 2(a), the aqueous phase emits brilliant red light surround dark oil droplets, confirming that the Pickering HIPE is an o/w emulsion. The average droplet diameter was about 85 ±

11 μm. With this o/w emulsion as template, hydrophilic monomers such as AM could be dissolved in the continuous aqueous phase and used to synthesize a porous polymer.

In order to further understand the location of CALB-loaded polymersomes in the emulsion, they were dyed with Rhodamine B and CALB inside them was labelled with FITC. The Pickering emulsion HIPE-0 was observed with CLSM. It was found that the enzyme-loaded polymersomes were mainly concentrated at the oil-water interface and showed a bright red colour with light of wavelength 561 nm (Figure 2(b)). When the emulsion was exposed to light of wavelength 488 nm, FITC emitted bright green light (Figure 2(c)), which further demonstrated CALB had been loaded into the polymersomes and therefore immobilized at the oil-water interface. This also verifies that the enzyme would not be lost to the oil phase during emulsification.

With HIPE-0 as a template, the macroporous polymer monolith was fabricated by adding both monomer AM and cross-linker MBAM to the aqueous phase before emulsification. Since the enzyme activity is temperature sensitive [44], a mild redox initiation composed of KPS and TMEDA was employed to fabricate the emulsion-templated polymeric monolith at 35 °C. After polymerization, water and *n*-heptane were removed by freeze-drying. As shown in Figure 3, the monolith had a closed-cell porous structure with an average void diameter of 86 ± 14 μm, similar to that of the Pickering HIPE templated polyHIPPEs in previous work [32, 45].

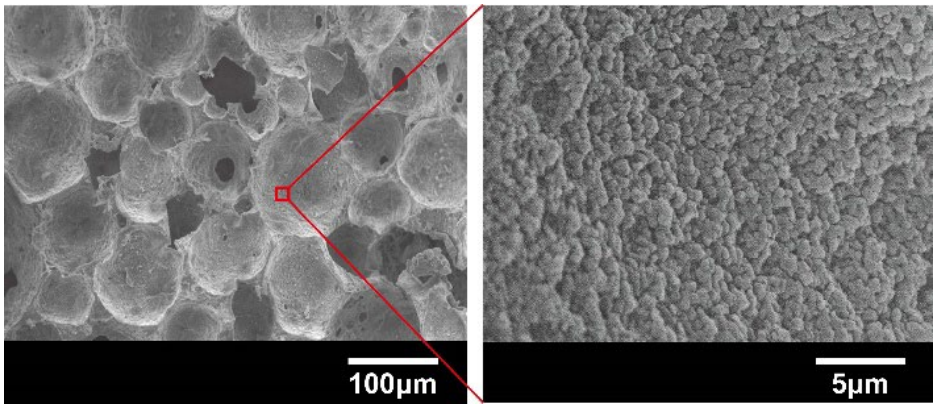


**Figure 3**. SEM images of porous polymer prepared from HIPE-0 template. Polymersomes can be seen on the surface of the voids (right).

Moreover, there was a large number of polymersomes on the void wall surface (Figure 3 right), meaning that the CALB-loaded polymersomes could be reached by the reaction substrate dissolved in a reaction medium inside the voids and therefore the resulting monolith is a potential solid biocatalyst and microreactor. The porosity of the monolith was 78.6 ± 1.4%.

To realize a flow-through and recyclable biocatalyst, a monolith having an open-cell porous structure is required. To form the interconnected pores between adjacent voids, addition of a small amount of surfactant as co-stabilizer has been shown to be an effective approach [32, 33, 46]. Herein, the surfactant Tween 85 of 2, 4 or 6 wt.% (with respect to the PBS buffer) was added to the aqueous phase as a co-stabilizer of the Pickering HIPEs before emulsification (named HIPE-2, HIPE-4 or HIPE-6). Although this surfactant cannot stabilize the HIPE alone, it will concentrate on the contact point between adjacent droplets and induce the formation of interconnected pores in the resulting porous materials during the curing process [33, 46].

Compared with the HIPE-0 that was stabilized solely by polymersomes (Figure 2(a)), HIPEs prepared in the presence of Tween 85 had a much smaller droplet size [47] which decreased from 23 ± 4.2 to 17 ± 3.4 and 10 ± 2.1 μm upon increasing the surfactant concentration from 2 to 4 to 6 wt.% (Figure 4(a)-(c)). They were all o/w type and stable to coalescence and creaming at room temperature for more than 20 days (Figure S9), which meant that they were also stable enough to be emulsion templates for preparing monoliths. Copolymerizing AM and MBAM in the aqueous phase of HIPE-2, HIPE-4 and HIPE-6 produced monoliths PPH-2, PPH-4 and PPH-6, respectively. The PPHs have an open-cell porous structure (Figure 4(d)-(f)). The average void size is similar to the droplet size of their precursor emulsions, since the voids are considered as a duplication of the droplets in emulsion templates [48]. The interconnectivity I of PPH-2, PPH-4 and PPH-6 calculated from the SEM images were 12.2 ± 2.1%, 18.0 ± 2.6% and 45.2 ± 6.8%, respectively, which are higher than those (4.8%-11.1%) of reported polyHIPPEs stabilized by both particles and surfactant [46].

The high interconnectivity of these monoliths makes them an ideal flow-through microreactor.

Besides, the mechanical strength of the monolith was characterized by measuring the compressive strength (Figure S10). The Young's modulus *E* was 107.5 KPa, which is higher than those of porous foams in previous work such as nanocellulose foams (17.3 kPa) and metal-organic polyhedral-based porous materials (11.0 kPa) [49, 50].

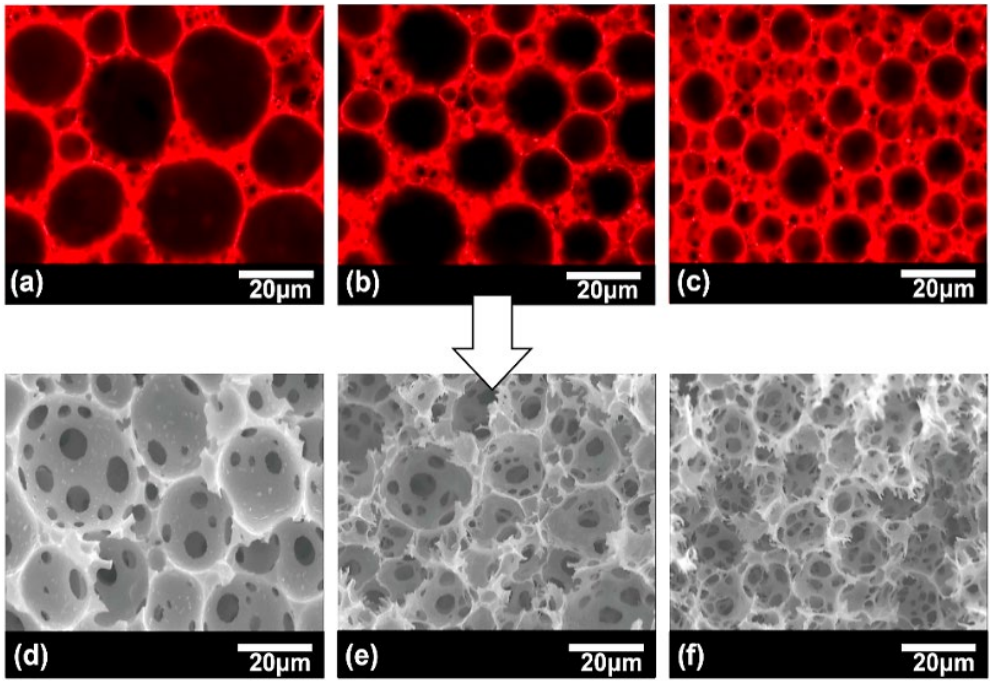


**Figure 4.** CLSM images of o/w Pickering HIPEs with different contents of Tween 85: (a) HIPE-2, (b) HIPE-4, (c) HIPE-6. Average diameter of droplets is (a) 23 μm, (b) 17 μm, (c) 10 μm. SEM images of the corresponding porous monoliths: (d) PPH-2, (e) PPH-4, (f) PPH-6.

### 3.3 Catalytic activity of monolithic catalyst

In order to verify the biocatalytic performance of the enzyme-loaded monoliths, the obtained open-cell PPH monoliths were used as bioreactors to carry out flow-through biphasic biocatalysis. A circulating flow catalytic system was established for the ongoing hydrolysis of *p*-NPB, and two immiscible phases of *p*-NPB in *n*-heptane and

PBS buffer were pre-added in a conical flask (Figure S11). Biocatalysis started when the upper oil phase containing *p*-NPB was pumped onto the top of the column and allowed to flow through the monolith driven by gravity. After all the oil phase was added, PBS buffer was then pumped onto the monolith to take out both the *n*-heptane and water-soluble product *p*-NP to the flask below the column. Phase separation occurred quickly between *n*-heptane and PBS buffer as they were collected in the flask. The emulsion-templated monolith, having a highly interconnected porous structure, has been proven to be a highly efficient micromixer for both emulsification and liquid-liquid extraction [35, 36, 51] which allowed the oil phase and product *p*-NB in the monolith to be washed out. Therefore, at the beginning of each loop, the substrate solution did not contain the product *p*-NP, which is conducive to the enzymatic hydrolysis reaction of *p*-NPB. Repeating the loop above enabled the biocatalysis to be continuous in the bioreactor. This catalytic process in the monolith is a solid emulsion-like interfacial catalysis and the polymersome provided a micro-catalytic space in which the substrate *p*-NPB could enter and be transformed into *p*-NP catalysed by CALB. The water-soluble *p*-NP was collected in PBS buffer.

As control experiments, the catalytic activity of the polyHIPPE (Figure S13) prepared using polymersomes without CALB was assessed in the same way used to determine the enzyme specific catalytic activity of polyHIPPEs prepared with CALB-loaded polymersomes. The hydrolytic conversion of *p*-NPB in the presence of free enzyme was also determined by shaking the two phases of PBS buffer containing CALB and *n*-heptane containing *p*-NPB at room temperature. The amount of generated *p*-NP was detected by measuring the absorbance at $\lambda = 405$ nm and calculated according to the calibration curve (Figure S12). As shown in Figure 5(a), the hydrolysis reaction reached equilibrium within 8 h in the presence of either free enzyme or enzyme contained within monoliths. Compared to the equilibrium conversion of 11.5% for free enzyme and no conversion for polyHIPPEs prepared using polymersomes without CALB, CALB-loaded PPHs exhibited a significant improvement reaching conversions of 33.2 ± 1.2%, 47.5 ± 1.5% and 67.9 ± 1.6% in monoliths PPH-2, PPH-4 and PPH-6,

respectively. Furthermore, as shown in Figure 5(b), specific activities of CALB in PPHs were much higher than that of free CALB. Taking PPH-6 for example, the specific activity was nearly 6 times that of free enzyme demonstrating improved interfacial biocatalysis for the monolith.

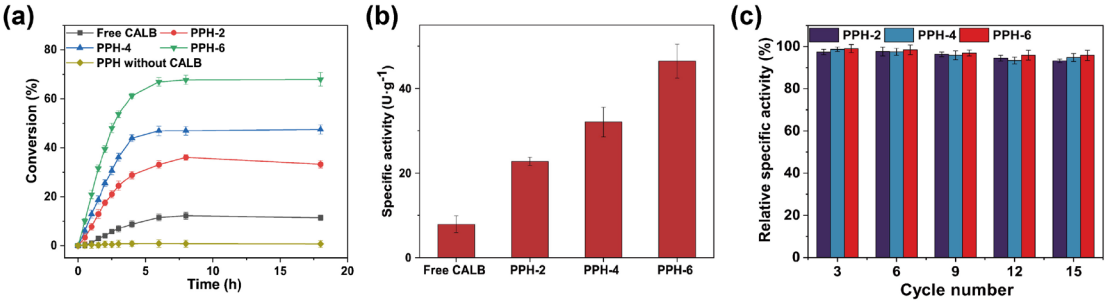


**Figure 5.** Catalytic performance of free CALB, CALB within polymersomes contained within monoliths (PPH-2, PPH-4, PPH-6) and monolith containing polymersomes devoid of CALB. (a) Time-dependent conversion of *p*-NPB to *p*-NP, (b) specific activities of enzyme. (c) Relative specific activity during recycling during the hydrolysis of *p*-NPB in PPH-2, PPH-4 and PPH-6 monoliths.

Considering all the bioreactors contain the same amount of CALB-loaded polymersomes and the higher specific activity of PPH-6 compared to that of PPH-2 and PPH-4, we can conclude that the higher enzyme specific activities of the monolith were due to improved substrate diffusion attributed to the greater interconnectivity I [52, 53]. Bioreactor PPH-6 had the highest interconnectivity (Table S1), which results in easier diffusion of both substrate and product inside the monolith, and we have shown that the significant substrate permeability of PPHs facilitated the contact of substrate and enzyme on the void wall leading to increased enzyme specific activity.

### 3.4 Recyclability of CALB-loaded monolith

To investigate the recyclability of CALB-loaded monoliths, we performed 15 hydrolysis cycles with the same monolith. After each catalytic experiment, the

monolith which was light yellow (Figure S14(b)) was recovered by rinsing with excess PBS buffer reverting to a white one (Figure S14(c)) like the pristine monolith before reaction (Figure S14(a)). Then the refreshed white monolith was used for a new cycle of enzymatic hydrolysis. It was found that owing to the stable insertion of both polymersomes and enzyme in monoliths as well as favourable microhabitats for CALB inside the polymersomes, the monoliths maintained their enzyme specific activity of over 93% in 15 cycles (Figure 5(c)). This means that the enzyme is constantly present in the microenvironment of the PBS buffer, which ensures its immunity to inactivation and facilitates its recycling. These results prove that CALB-loaded monoliths can be a highly effective and recyclable bioreactor for flow-through enzymatic reactions.

**4. Conclusions**

We have designed an effective and recyclable interfacial enzyme catalysis system for multiple cycling of an enzymatic reaction templated by a CALB-loaded polymersome-stabilized Pickering emulsion. In this process, an amphiphilic diblock copolymer $PEO_{44}$-*b*-P($St_{79}$-*co*-$TMI_4$) was synthesized to be a building block for constructing CALB-loaded polymersomes. After the polymersomes were strengthened by cross-linking, they acted as both the stabilizer of the emulsion template and the enzymatic reaction site on the void surface of the resulting monolith. Regardless of the external environment, the PBS buffer microenvironment of the polymersomes maintained the integrity of the enzyme. When the monolith was used as a bioreactor for high-throughput enzymatic hydrolysis of *p*-NPB, a high conversion rate along with high specific activity of CALB were achieved. The open-cell porous structure of the monolith allowed the reaction substrate to reach the reaction site, and the catalytic efficiency increased with an increase in the material interconnectivity. The biphasic interfacial biocatalytic microreactors maintained their enzyme specific activities of over 93% in 15 cycles, which is higher than the reported microchannel bioreaction systems such as the glass-polydimethylsiloxane groove-typed channel microreactor

which cross-links to immobilize enzymes with 56% residual activity after 12 cycles [54], reflecting excellent enzymatic catalytic activity and re-usability of the monolith. Therefore, a high-throughput microchannel bioreactor with tuneable interconnectivity for improved biocatalytic performance and long-term stability of enzymes has been developed successfully. The prepared immobilized enzyme microchannel reactor has great potential in cascade biocatalytic reactions with immobilization of different enzymes.

## Data availability

A detailed explanation of the methods is provided in the Supporting Information. The data that support the findings of this study are available from the corresponding authors upon reasonable request.

## CRediT authorship contribution

Zhengqiao Yin: Methodology, Software, Investigation, Data curation, Writing- Original draft; Yiding Zhou: Investigation, Formal analysis; Xiucai Liu: Writing- Reviewing and Editing; Shengmiao Zhang: Conceptualization, Supervision, Methodology, Funding acquisition, Writing- Reviewing and Editing; Bernard P. Binks: Supervision, Writing- Reviewing and Editing.

## Conflicts of interest

There are no conflicts to declare.


## Acknowledgements

This research was supported by the National Natural Science Foundation of China (51773059) and the Natural Science Foundation of Shanghai (16ZR1407800).

## References


[1] U.T. Bornscheuer, G.W. Huisman, R.J. Kazlauskas, S. Lutz, J.C. Moore, K. Robins, Engineering the third wave of biocatalysis, *Nature* **485** (2012) 185-94.

[2] F. Chang, C.M. Vis, W. Ciptonugroho, P.C.A. Bruijnincx, Recent developments in catalysis with Pickering Emulsions, *Green Chem*. **23** (2021) 2575-2594.

[3] A.M. Bago Rodriguez, L. Schober, A. Hinzmann, H. Groger, B.P. Binks, Effect of Particle Wettability and Particle Concentration on the Enzymatic Dehydration of n-Octanaloxime in Pickering Emulsions, *Angew. Chem. Int. Ed*. **60** (2021) 1450-1457.

[4] Y. Xi, B. Liu, S. Wang, X. Huang, H. Jiang, S. Yin, T. Ngai, X. Yang, Growth of Au nanoparticles on phosphorylated zein protein particles for use as biomimetic catalysts for cascade reactions at the oil–water interface, *Chem. Sci*. 12 (2021) 3885-3889.

[5] X. Yang, Y. Wang, R. Bai, H. Ma, W. Wang, H. Sun, Y. Dong, F. Qu, Q. Tang, T. Guo, B.P. Binks, T. Meng, Pickering emulsion-enhanced interfacial biocatalysis: tailored alginate microparticles act as particulate emulsifier and enzyme carrier, *Green Chem*. **21** (2019) 2229-2233.

[6] U. Hanefeld, L. Gardossi, E. Magner, Understanding enzyme immobilisation, *Chem. Soc. Rev*. **38** (2009) 453-468.

[7] J. Lei, L. Qi, Z. Luo, Pickering Emulsion-Based Microreactors for Size-Selective Interfacial Enzymatic Catalysis, *Front. Bioeng. Biotech*. **8** (2020) 950.

[8] Z. Sun, U. Glebe, H. Charan, A. Boker, C. Wu, Enzyme-Polymer Conjugates as Robust Pickering Interfacial Biocatalysts for Efficient Biotransformations and One-Pot Cascade Reactions, *Angew. Chem. Int. Ed*. **57** (2018) 13810-13814.

[9] M. Wang, M. Wang, S. Zhang, J. Chen, Pickering gel emulsion stabilized by enzyme immobilized polymeric nanoparticles: A robust and recyclable biocatalyst system for biphasic catalysis, *React. Chem. Eng*. **4** (2019) 1459-1465.

[10] Z. Wang, M.C. van Oers, F.P. Rutjes, J.C. van Hest, Polymersome colloidosomes for enzyme catalysis in a biphasic system, *Angew. Chem. Int. Ed*. **51** (2012) 10746-10750.

[11] M. Miyazaki, H. Maeda, Microchannel enzyme reactors and their applications for processing, *Trends Biotechnol*. **24** (2006) 463-470.

[12] R.A. Sheldon, S. van Pelt, Enzyme immobilisation in biocatalysis: why, what and how, *Chem. Soc. Rev*. **42** (2013) 6223-6235.

[13] A.I. Benitez-Mateos, S. Bertella, J. Behaghel de Bueren, J.S. Luterbacher, F. Paradisi, Dual Valorization of Lignin as a Versatile and Renewable Matrix for Enzyme Immobilization and (Flow) Bioprocess Engineering, *ChemSusChem* **14** (2021) 3198-3207.

[14] T. Honda, M. Miyazaki, H. Nakamura, H. Maeda, Immobilization of enzymes on a microchannel surface through cross-linking polymerization, *Chem. Commun*. **40** (2005) 5062-5064.

[15] T. Honda, M. Miyazaki, H. Nakamura, H. Maeda, Facile preparation of an enzyme-immobilized microreactor using a cross-linking enzyme membrane on a microchannel surface, *Adv. Synth. Catal*. **348** (2006) 2163-2171.

[16] A.M. Hickey, L. Marle, T. McCreedy, P. Watts, G.M. Greenway, J.A. Littlechild, Immobilization of thermophilic enzymes in miniaturized flow reactors, *Biochem. Soc. T*. **35** (2007) 1621-1623.

[17] R. Tarasi, M. Alipour, L. Gorgannezhad, S. Imanparast, A. Yousefi-Ahmadipour, A. Ramezani, M.R. Ganjali, A. Shafiee, M.A. Faramarzi, M. Khoobi, Laccase Immobilization onto Magnetic beta-Cyclodextrin-Modified Chitosan: Improved Enzyme Stability and Efficient Performance for Phenolic Compounds Elimination, *Macromol. Res*. **26** (2018) 755-762.

[18] J. Qiao, L.L. Liu, J. Shen, L. Qi, Enzyme immobilization on a pH-responsive porous polymer membrane for enzymatic kinetics study, *Chin. Chem. Lett*. **32** (2021) 3195-3198.

[19] Y. Ning, Y. Yang, C.Y. Wang, T. Ngai, Z. Tong, Hierarchical porous polymeric microspheres as efficient adsorbents and catalyst scaffolds, *Chem. Commun*. **49** (2013) 8761-8763.

[20] Y. Huang, L. Tan, M. Chen, Y. Jiao, J. Tian, L. Li, C. Zhou, L. Lu, Laccase

immobilization on hierarchical micro/nano porous chitin/graphene oxide beads prepared via Pickering emulsion template for dye decolorization, *Colloids Surf. A* **661** (2023) 130858.

[21] C. Xu, Y. Sun, Y. Sun, R. Cai, S. Zhang, High Internal Phase Pickering Emulsion Stabilized by Lipase-Coated ZIF-8 Nanoparticles towards Recyclable Biphasic Biocatalyst, *Catalysts* **13** (2023) 383.

[22] M. Wang, M. Wang, Y. Zhu, S. Zhang, J. Chen, Enzyme immobilized millimeter-sized polyHIPE beads with easy separability and recyclability, *React. Chem. Eng*. **4** (2019) 1136-1144.

[23] N.R. Cameron, High internal phase emulsion templating as a route to well-defined porous polymers, *Polymer* **46** (2005) 1439-1449.

[24] H. Zhang, A.I. Cooper, Synthesis and applications of emulsion-templated porous materials, *Soft Matter* **1** (2005) 107-113.

[25] S.M. Zhang, J.D. Chen, PMMA based foams made via surfactant-free high internal phase emulsion templates, *Chem. Commun*. **16** (2009) 2217-2219.

[26] V.O. Ikem, A. Menner, A. Bismarck, High internal phase emulsions stabilized solely by functionalized silica particles, *Angew. Chem. Int. Ed*. **47** (2008) 8277-8279.

[27] J. Xu, X. Chen, Mixing performance of a fractal-like tree network micromixer based on Murray's law, *Int. J. Heat Mass Transf.* **141** (2019) 346-352.

[28] M. Zhang, L. Wei, H. Chen, Z. Du, B.P. Binks, H. Yang, Compartmentalized Droplets for Continuous Flow Liquid-Liquid Interface Catalysis, *J. Am. Chem. Soc*. **138** (2016) 10173-10183.

[29] W. Jiang, Y. Zhou, D. Yan, Hyperbranched polymer vesicles: from self-assembly, characterization, mechanisms, and properties to applications, *Chem. Soc. Rev*. **44** (2015) 3874-3889.

[30] B.M. Discher, Y.Y. Won, D.S. Ege, J.C.M. Lee, F.S. Bates, D.E. Discher, D.A. Hammer, Polymersomes: Tough vesicles made from diblock copolymers, *Science* **284** (1999) 1143-1146.

[31] A. Eyigor, F. Bahadori, V.B. Yenigun, M.S. Eroglu, Beta-Glucan based temperature responsive hydrogels for 5-ASA delivery, *Carbohydr. Polym*. **201** (2018) 454-463.

[32] V.O. Ikem, A. Menner, T.S. Horozov, A. Bismarck, Highly permeable macroporous polymers synthesized from Pickering medium and high internal phase emulsion templates, *Adv. Mater*. **22** (2010) 3588-3592.

[33] Y. Hua, S.M. Zhang, Y. Zhu, Y.Q. Chu, J.D. Chen, Hydrophilic polymer foams with well-defined open-cell structure prepared from pickering high internal phase emulsions, *J. Polym. Sci. Pol. Chem*. **51** (2013) 2181-2187.

[34] Y. Hua, S.M. Zhang, J.D. Chen, Y. Zhu, Switchable release and recovery of nanoparticles via a Pickering-emulsion-templated porous carrier, *J. Mater. Chem*. *A* **1** (2013) 13970-13977.

[35] H. Barkan-Öztürk, A. Menner, A. Bismarck, Polymerised high internal phase emulsion micromixers for continuous emulsification, *Chem. Eng. Sci*. **252** (2022) 117296.

[36] H. Barkan-Oeztuerk, A. Menner, A. Bismarck, Emulsion-Templated Macroporous Polymer Micromixers, *Ind. Eng. Chem. Res*. **60** (2021) 14013-14025.

[37] B. Vanhaecht, M.N. Teerenstra, D.R. Suwier, C.E. Koning, Dicyclohexylcarbodiimide Assisted Synthesis of Aliphatic Polyesters at Room Temperature, *J. Macromol. Sci. A* **37** (2000) 633-643.

[38] J. Bang, S.H. Kim, E. Drockenmuller, M.J. Misner, T.P. Russell, C.J. Hawker, Defect-free nanoporous thin films from ABC triblock copolymers, *J. Am. Chem. Soc*. **128** (2006) 7622-7629.

[39] Z. Song, Y. Huang, V. Prasad, R. Baumgartner, S. Zhang, K. Harris, J.S. Katz, J. Cheng, Preparation of Surfactant-Resistant Polymersomes with Ultrathick Membranes through RAFT Dispersion Polymerization, *ACS Appl. Mater. Interfaces* **8** (2016) 17033-17037.

[40] P.L. Soo, A. Eisenberg, Preparation of block copolymer vesicles in solution, *J. Polym. Sci. Pol. Phys*. **42** (2004) 923-938.

[41] K.L. Thompson, P. Chambon, R. Verber, S.P. Armes, Can polymersomes form

colloidosomes?, *J. Am. Chem. Soc*. **134** (2012) 12450-12453.

[42] A. Clemente, R. Jimenez, M.M. Encabo, M.P. Lobera, F. Balas, J. Santamaria, Fast and simple assessment of surface contamination in operations involving nanomaterials, *J. Hazard. Mater*. **363** (2019) 358-365.

[43] J. Wu, X. Guan, C. Wang, T. Ngai, W. Lin, pH-Responsive Pickering high internal phase emulsions stabilized by Waterborne polyurethane, *J. Colloid Interface Sci*. **610** (2021) 994-1004.

[44] M. Shahedi, M. Yousefi, Z. Habibi, M. Mohammadi, M.A. As'habi, Co-immobilization of Rhizomucor miehei lipase and Candida antarctica lipase B and optimization of biocatalytic biodiesel production from palm oil using response surface methodology, *Renew. Energy* **141** (2019) 847-857.

[45] Y. Zhu, S.M. Zhang, Y. Hua, H. Zhang, J.D. Chen, Synthesis of Latex Particles with a Complex Structure As an Emulsifier of Pickering High Internal Phase Emulsions, *Ind. Eng. Chem. Res*. **53** (2014) 4642-4649.

[46] W. Zhu, Y. Zhu, C. Zhou, S. Zhang, Pickering emulsion-templated polymers: insights into the relationship between surfactant and interconnecting pores, *RSC Adv*. **9** (2019) 18909-18916.

[47] Y. Hua, Y.P. Li, S.M. Zhang, J.D. Chen, V.T. Perchyonok, Synergistic Effect of Copolymer Particle and Surfactant on the Morphology of Macroporous Materials Based on High Internal Phase Emulsion, *Curr. Org. Chem*. **16** (2012) 2415-2422.

[48] T. Zhang, R.A. Sanguramath, S. Israel, M.S. Silverstein, Emulsion Templating: Porous Polymers and Beyond, *Macromolecules* **52** (2019) 5445-5479.

[49] M. Mariano, L.W. Hantao, J.D. Bernardes, M. Strauss, Microstructural characterization of nanocellulose foams prepared in the presence of cationic surfactants, *Carbohydr. Polym*. **195** (2018) 153-162.

[50] A. Legrand, G.A. Craig, M. Bonneau, S. Minami, K. Urayama, S. Furukawa, Understanding the multiscale self-assembly of metal-organic polyhedra towards functionally graded porous gels, *Chem. Sci*. **10** (2019) 10833-10842.

[51] H. Barkan-Oeztuerk, J. Delorme, A. Menner, A. Bismarck, Liquid-liquid

extraction using combined hydrophilic-hydrophobic emulsion templated macroporous polymer micromixer-settlers, *Chem. Eng. Process. Process Intensif*. **181** (2022) 109153.

[52] H. Gu, Y. Liu, L. Wang, B. Zhang, D. Yin, Q. Zhang, Monolithic macroporous hydrogels prepared from oil-in-water high internal phase emulsions for high-efficiency purification of Enterovirus 71, *Chem. Eng. J*. **401** (2020) 126051.

[53] S. Currivan, J.M. Macak, P. Jandera, Polymethacrylate monolithic columns for hydrophilic interaction liquid chromatography prepared using a secondary surface polymerization, *J. Chromatogr. A* **1402** (2015) 82-93.

[54] C.T. Zhu, A. Gong, F. Zhang, Y. Xu, S. Sheng, F.A. Wu, J. Wang, Enzyme immobilized on the surface geometry pattern of groove-typed microchannel reactor enhances continuous flow catalysis, *J. Chem. Technol. Biotechnol*. **94** (2019) 2569-2579.